Journal of Magnetic Resonance **139,** 281–286 (1999)
Article ID jmre.1999.1769, available online at http://www.idealibrary.com on IDEAL®

Nitroxide Side-Chain Dynamics in a Spin-Labeled Helix-Forming Peptide Revealed by High-Frequency (139.5-GHz) EPR Spectroscopy

M. Bennati,* G. J. Gerfen,† G. V. Martinez,‡ R. G. Griffin,*,§ D. J. Singel,¶ and G. L. Millhauser‡,[1]

‡*Department of Chemistry and Biochemistry, University of California, Santa Cruz, California 95064;* **Francis Bitter Magnet Laboratory and* §*Department of Chemistry, Massachusetts Institutes of Technology, Cambridge, Massachusetts 02139;* ¶*Department of Chemistry and Biochemistry, Montana State University, Bozeman, Montana 59717; and* †*Department of Physiology and Biophysics, Albert Einstein College of Medicine, 1300 Morris Park Avenue, Bronx, New York 10461*

Received November 18, 1998; revised March 31, 1999

High-frequency electron paramagnetic resonance (EPR) spectroscopy has been performed on a nitroxide spin-labeled peptide in fluid aqueous solution. The peptide, which follows the single letter sequence

Ac-(AAAAK)$_2$CAAAKA-NH$_2$ 3K-11,

was reacted with the methanethiosulfonate spin label at the cysteine sulfur. The spin sensitivity of high-frequency EPR is excellent with less than 20 pmol of sample required to obtain spectra with good signal-to-noise ratios. Simulation of the temperature-dependent spectral lineshapes reveals the existence of local anisotropic motion about the nitroxide N–O bond with a motional anisotropy $\tau_\perp/\tau_\parallel$ ($\equiv$ N) approaching 2.6 at 306 K. Comparison with previous work on rigidly labeled peptides suggests that the spin label is reorienting about its side-chain tether. This study demonstrates the feasibility of performing 140-GHz EPR on biological samples in fluid aqueous solution. © 1999 Academic Press

Key Words: **EPR; peptide; high frequency; side-chain dynamics; anisotropic motion.**

INTRODUCTION

Understanding the structure and dynamic properties of peptides is of pressing interest in chemistry, biochemistry, and biotechnology. Although there are a number of spectroscopic methodologies useful for exploring peptides, spin-label electron paramagnetic resonance (EPR) has proven to be a powerful probe of these features. EPR methods have been used to rank distances between side chains in doubly labeled peptides thereby suggesting local folding geometry (*1–4*). Moreover, recent work has demonstrated that EPR of site-specific spin-labeled peptides is excellent at revealing position-dependent dynamics (*5, 6*). For example, in an alanine-based helical peptide, EPR demonstrates that structure at the C-terminus is substantially more dynamic than at the N-terminus (*7*). These studies provide information that is critical in the development of new conceptual models of peptide structure and dynamics (e.g., see Refs. *8,–10*).

[1] To whom correspondence should be addressed. Fax: (831) 459-2935. E-mail: glennm@hydrogen.ucsc.edu.

Although these EPR experiments have added considerably to our understanding of peptide motions, many important details remain unresolved. In particular, we have found that 9-GHz EPR spectra are not particularly sensitive to the anisotropy of the spin-label motion (*11*). Thorough characterization of the local-label motion is necessary in order to clarify the interpretation of the position-dependent dynamics and to aid in the determination of distances in double-label experiments. In addition, characterization of label motion should prove useful in the emerging field of site-directed spin labeling (*5, 12–14*).

It has been recognized that high-frequency EPR spectra (95 GHz or greater) are more sensitive than 9-GHz spectra to the anisotropy of molecular motion particularly in the short correlation time regime (*15, 16*). Here we report the utilization of 139.5-GHz EPR to study a spin-labeled peptide in fluid aqueous solution. We find that the high-frequency spectra are sensitive to anisotropic motion but remain amenable to simple lineshape analysis. These benefits are obtained without compromising sensitivity: spectra were obtained with 20 pmol of labeled peptide (20 nL of a 1.2-mM sample), thus rivaling the signal-to-noise limit of modern loop gap resonators operating at 9 GHz (*12*). The results of this study also illustrate important benefits that high-frequency EPR offers for the study of spin-labeled biopolymers in aqueous solution.

The subject peptide in this study is the alanine-based sequence

Ac-AAAAKAAAAKCAAAKA-NH$_2$ [3K-11,]

where we have used the single-letter amino acid code (A, Ala; K, Lys; C, Cys) (*7*). Labeling is accomplished with the methanethiosulfonate spin label (MTSSL), which attaches specifically to the sulfur of the Cys residue giving a Cys-SL side chain as shown in Fig. 1 (*11, 17*). Also shown is the coordinate system for describing motion about the nitroxide molecular axes. The 3K-11 peptide is largely helical in aqueous solution at 1°C, as determined by circular dichroism. An illustration of this peptide in a helical conformation is shown in the lower panel of Fig. 1.

1090-7807/99 $30.00

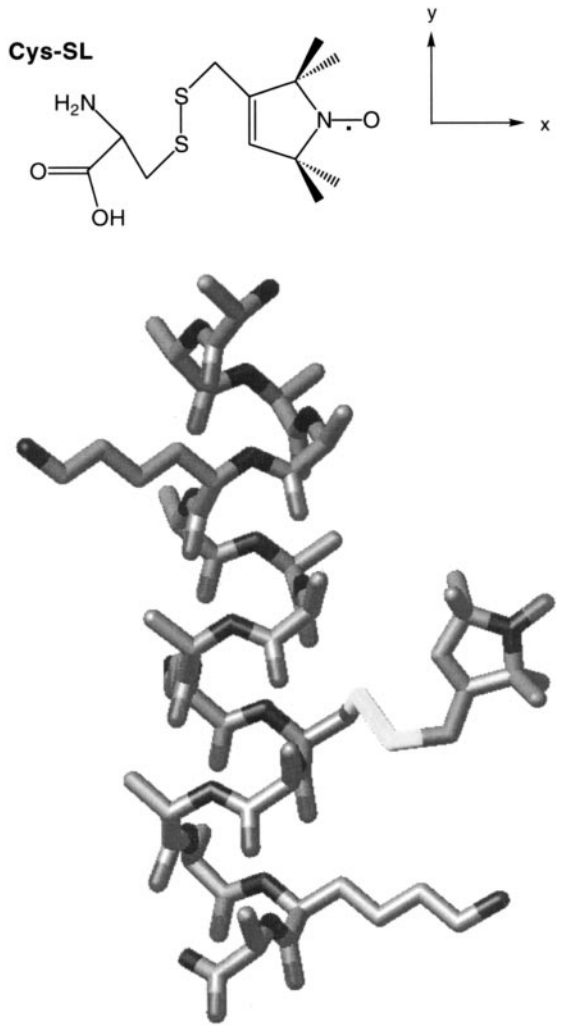

FIG. 1. (Top) The Cys-SL side chain showing the nitroxide coordinates. The *z* axis is perpendicular to the C–N–C plane of the nitroxide. (Bottom) The spin-labeled, 16-residue 3K-11 peptide. The disulfide linker between the peptide and the nitroxide is shown with light shading and tucked up against the helix barrel in a manor suggested by Mchaourab *et al.* (*38*).

MATERIALS AND METHODS

The 3K-11 peptide was synthesized by the solid-phase method as described elsewhere (*7*). After the peptides were cleaved from the resin with neat trifluoroacetic acid, they were purified by preparative HPLC. Mass spectra determinations gave the expected values for both the unlabeled and the labeled peptide. The molecular model was built and examined using the MolMol (*18*) and Rasmol (*19*) programs.

The 139.5-GHz spectrometer has been described previously (*20*). Samples contained 20 nL of 1.2-mM peptide (20 pmol) in aqueous buffer (Mops) at pH 7. Aqueous samples were drawn into a 0.1-mm-inner-diameter capillary, examined with a light microscope to insure proper filling of the capillary, and mounted into the center of a cylindrical resonator. Sample temperature was controlled with externally heated nitrogen gas flow and monitored with a Lake Shore silicon diode sensor.

Rigid lattice spectra were simulated using a program developed by one of us (M.B.) in the MATLAB language using a standard formalism for orientation-dependent electron spin transitions (e.g., see Ref. *21*). Line broadening was included by convoluting the calculated stick spectrum with a Gaussian lineshape function.

RESULTS

Measurement of Magnetic Tensors

To obtain rigid lattice *g* and *A* tensor values for the Cys-SL reporter, we recorded spectra from a sample of 3K-11 dissolved in ethanol and cooled to 120 K. The magnetic field was calibrated with an ^{2}H lock system (*22*). The experimental spectrum together with simulations is shown in Fig. 2. The signal-to-noise is excellent ($S/N > 100$) and dominance of the *g* tensor at high field allows for highly accurate determination of its values. It was assumed, as is typical for nitroxides, that the principal axes of **g** and **A** are coincident and we defined the *x*, *y*, and *z* magnetic axes as belonging to the largest through smallest *g* values, in which case the *z* axis also belongs to the largest principal value of the hyperfine interaction tensor. Simulations were performed to estimate **g** and **A** and the results are reported in Table 1. The *g* tensor and A_{zz} are well constrained by the fits. However, A_{xx} and A_{yy} are small compared to A_{zz} and result mainly in broadening of the g_{xx} and g_{yy} edges of the powder lineshape. We approximated $A_{xx} = A_{yy}$ (which is typical for nitroxides) and Gaussian inhomogeneous broadening of 9.0 G and found that spectra computed with A_{xx}, A_{yy} ranging from 4.9 to 6.0 G gave excellent simulations of the experimental spectrum (Fig. 2) in agreement with Ref. (*16*). The resulting tensor values compare well with those previously determined at 9 GHz (Table 1).

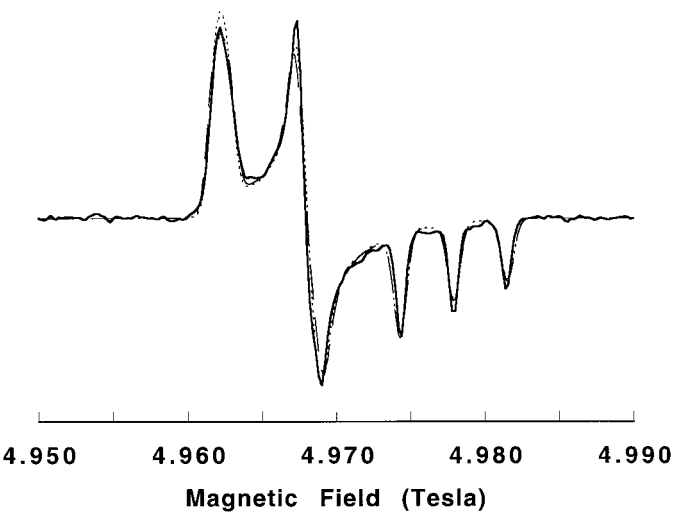

FIG. 2. Frozen solution spectrum of the 3K-11 in ethanol at 120 K (solid line). Simulations using the parameters in Table 1 are overlaid with $A_{xx} = A_{yy} = 4.9$ G (short dashes) and $A_{xx} = A_{yy} = 6.0$ G (long dashes).

TABLE 1
Magnetic Parameters Determined for the Cys-SL Side Chain

	139.5 GHz[a]	9.4 GHz[b,c]
g_{xx}	2.00848	2.0086
g_{yy}	2.00610	2.0066
g_{zz}	2.00217	2.0032
A_{xx}	6.0 G	6.23 G
A_{yy}	6.0 G	6.23 G
A_{zz}	36.1 G	35.7 G

[a] g tensor values accurate to ± 0.00005.
[b] g tensor values determined by Capiomont *et al.* (*42*).
[c] A tensor determined by Todd and Millhauser (*11*).

Determination of Temperature-Dependent τ_R and N in Aqueous Solution

Temperature-dependent spectra were recorded between 277 and 306 K and typical results are shown in Fig. 3. Each spectrum is an average of four scans with a modulation amplitude of 2.5 G. (Note that the narrowest peak-to-peak linewidth among these spectra is 4 G for the 306-K low field line.) The spectra at the higher temperatures exhibit the characteristic three-line hyperfine pattern of a motionally narrowed nitroxide. The spectra at 277 and 285 K appear to be more complex because the hyperfine lines are broader, with linewidths comparable to the isotropic hyperfine interaction. Nevertheless, a qualitative comparison of these lineshapes reveals a significant sensitivity to temperature and therefore the correlation time (τ_R) of the spin-labeled peptide can be assessed with some accuracy.

The criteria for valid application of motional narrowing theory in the interpretation of high-frequency spectra have been discussed by Freed and co-workers (*23*). Accordingly, all the spectra in Fig. 3 are amenable to analysis with simple motional narrowing theory, notwithstanding the apparent complexity of the spectra obtained at the lower temperatures. (As an additional check, this approach was verified with slow motional lineshape theory (*24*).) Within the motional narrowing regime, the width of the hyperfine line for nitrogen spin state M is determined by the relation

$$T_2^{-1}(M) = A + BM + CM^2, \qquad [1]$$

where the lineshape parameters A, B, and C depend on the correlation times for spin-label reorientation, the g and A tensors, and the resonance frequency. Reorientation is modeled as axially symmetric Brownian diffusion with correlation time $\tau_\parallel$ about the unique axis and $\tau_\perp$ about axes perpendicular to the unique axis. With these parameters the correlation time is defined as $\tau_R = (\tau_\parallel \tau_\perp)^{1/2}$ and the motional anisotropy is described by the relation $N = \tau_\perp/\tau_\parallel$.

Spectral simulations using linewidths calculated according to Eq. 1, with τ_R and N as adjustable parameters and $A_{xx} = A_{yy} = 6.0$ G (to match the isotropic hyperfine splitting), are overlaid on the experimental spectra in Fig. 3. Although inhomogeneous broadening arising from proton hyperfine interactions (0.9 G) has been included in simulations of the high-temperature spectra (*11*), the significant motionally dependent homogeneous broadening (approximately 4 G peak-to-peak width for the narrowest hyperfine line) of each hyperfine line renders this correction largely unnecessary. In addition, Heisenberg spin exchange is expected to contribute at most only 0.2 G to the homogeneous linewidth so this effect may also be ignored (*25*). The simulations shown represent the best least-squares fits between simulation and experiment as found by an automated simplex search procedure (*26*) with variation of τ_R and N. We examined models of isotropic motion ($\tau_\parallel = \tau_\perp$, $N = 1$) and anisotropic motion. In the case of anisotropic

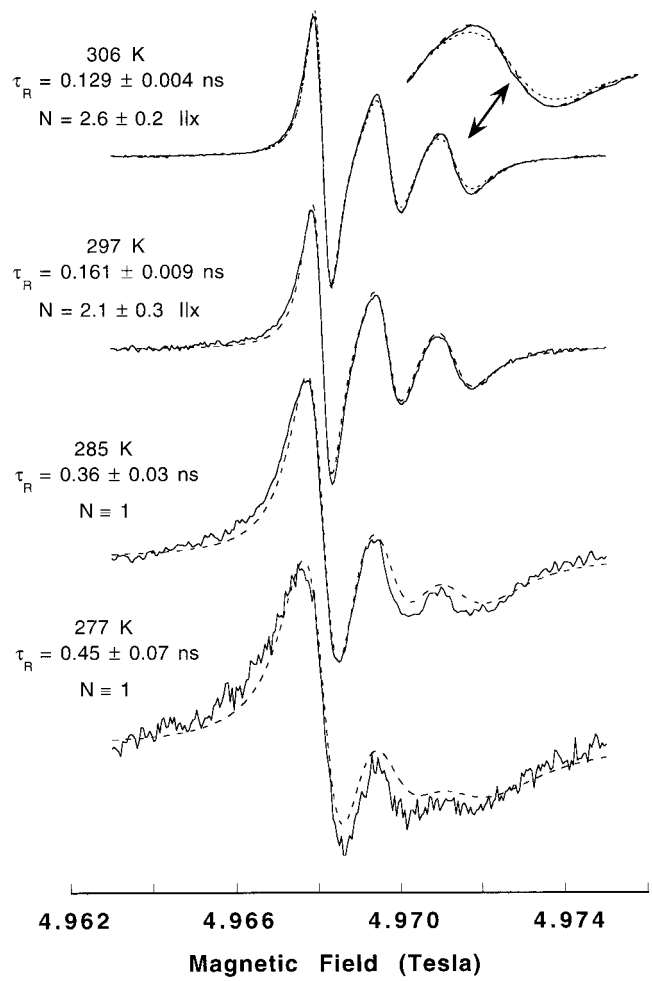

FIG. 3. Temperature-dependent EPR spectra (solid lines) and simulations (dashed lines) of the 3K-11 at 139.5 GHz. Additional acquisition parameters not reported in the text include time constant = 300 ms, sweep time = 5 min, and incident power = 200 μW. Parameters for the simulations as determined by least-squares spectra fits are given next to each spectrum. The two spectra obtained at the higher temperatures are best fit with a model of anisotropic motion. For comparison, both isotropic (short dashes) and anisotropic fits to 306-K spectrum are shown. The high field line is expanded to demonstrate the superior fit from the model of anisotropic motion.

motion, we assumed for simplicity that the unique axis lay parallel to one of the nitroxide principal axes in Fig. 1 and parametrically tested each of the three possibilities (i.e., the unique axes parallel to x, y, or z).

At the two higher temperatures, models of anisotropic motion with rapid reorientation about the x axis (parallel to the N–O bond) provide excellent fits to the spectra. A model of isotropic motion gave poorer fits at both 306 and 297 K and models of anisotropic motion with other choices for the unique axis provided reasonable fits but with $N < 1$. At 306 K, both the full spectrum and the inset showing the expanded high field line highlight the difference in fits between isotropic and anisotropic motion. Anisotropic motion with $N = 2.6$ is almost indistinguishable from the experimental spectrum. In contrast, isotropic motion gives a somewhat poorer fit especially to the central and high field lines. While the difference between the fits is not large, it nevertheless suggests that anisotropic motion provides a better model of the experimental data. For the 297 K data, we show only the fit to anisotropic motion. However, as found at 306 K, anisotropic motion provides a better fit to the data.

The spectra at the two lower temperatures were more difficult to analyze. Isotropic motion and anisotropic motion about the three possible axes were explored. Although we allowed the fitting routine to sample very large values of N, we found no model that provided better simulations than simple isotropic motion, at least as determined by the calculated residual and by visual inspection. The simulations for isotropic motion are shown in Fig. 3. While the calculated spectra do a reasonable job of reproducing the features of the low field line, details of the middle and high field components are not well simulated. Since at present no model was able to improve the fit over that obtained from isotropic motion, we assign the motion in this temperature regime as isotropic.

DISCUSSION

Analysis of the spectra suggest that at low temperature there is no evidence for anisotropic motion. However, at higher temperature, the motional anisotropy becomes resolvable and increases to 2.6 at 306 K. It is interesting to compare these data to those recently obtained from a 3K peptide spin labeled at position eight with the rigid nitroxide TOAC (*27*). TOAC is an unnatural, conformationally constrained nitroxide amino acid (*28–30*). Spectra for the TOAC-labeled peptides were obtained as a function of temperature and spectral fitting demonstrated the presence of significant anisotropic motion. However, in contrast to the findings presented here, N was found to be largest at 274 K and decreased monotonically as the temperature was increased. These data were interpreted as indicating anisotropic rotation of peptide about its helical axis, with decreasing anisotropy as the peptide thermally unfolds. In addition, we determined a correlation time of 2.6 ns at 274 K.

The experiments with a TOAC-labeled helical peptide demonstrate that a rigidly labeled helical peptide should give evidence of anisotropic motion. However, the data presented here indicate that under conditions that favor helix folding (low temperature) only isotropic motion is resolvable. In addition, the observed correlation time for the Cys-SL side chain is substantially shorter than that found for the rigidly labeled peptide. Thus, it appears that there may be motion of the Cys-SL side chain relative to the peptide on the nanosecond time scale.

It is interesting to consider the nature of these local motions by examining the results of solid state ^{2}H NMR studies of the dynamics of aromatic side chains. A number of ^{2}H lineshape and spin–lattice relaxation experiments have demonstrated millisecond to submicrosecond twofold ring flipping for Phe and Tyr residues in crystalline and membrane-bound peptides and proteins (*31–36*). A general trend revealed by these investigations is for systems with twofold symmetry, the barriers for motion are low and the correlation times for twofold motion are in the microsecond regime. However, as the twofold symmetry is broken, the barriers rise and the flipping rates drop dramatically. Thus, in Tyr-containing systems, where the ζ-OH breaks the twofold symmetry, it is necessary to achieve >100°C to obtain fast limit spectra. In Trp there is essentially no motion about the Cβ–Cγ bond. Based on these observations we do not expect the five-member nitroxide ring to execute twofold flips at a rate that will significantly average the g or A tensors. This assumption could be checked by examining the ^{2}H spectrum of MTSSL samples containing –CD_3 groups. Thus, any motional averaging of the nitroxide spectrum is likely due to cumulative librations about the five bonds intervening between the Cα and the five-member nitroxide ring.

The results presented here suggest that the nitroxide side chain is experiencing motion that is more rapid than the peptide tumbling motions. In addition, at higher temperature, the motion may be anisotropic and this could arise from motion about the nitroxide tether. Steinhoff and Hubbell have used Brownian dynamics calculations to characterize conformations and motions of the Cys-SL side chain when attached to the surface of a helix (*37*). Their work suggests that the nitroxide adopts several distinct low-energy conformations within the helix frame and jumps among these conformations with a correlation time of 500 ps. While lingering in any of these conformations, the nitroxide undergoes rapid, picosecond librations of 14 to 23°. EPR spectra calculated from these dynamics trajectories do an excellent job of reproducing experimental spectra obtained from spin-labeled bacteriorhodopsin.

The concepts brought forth by Steinhoff and Hubbell suggest an explanation for our results on the 3K-11 peptide. At low temperature, the label is partially immobilized against the barrel of the peptide helix. The nitroxide side chain takes on multiple conformations, each of which is in a different orientation with respect to the helix axis. The peptide may tumble anisotropically, as found by Hanson *et al.* (*27*), but because the nitroxide does not assume a preferred orientation with respect to the helix axis, the nitroxide motion appears isotropic. To test this hypothesis, three spectra were simulated each with aniso-

tropic motion ($N = 5$) about one of the unique nitroxide axes. The individual anisotropic spectra were summed and the resulting spectrum was found to be nearly indistinguishable from a spectrum calculated according to simple isotropic motion with the same correlation time (data not shown). That we did not obtain an exact match to isotropic motion for the low-temperature spectra may reflect the fact that individual conformations may experience different local environments and, hence, different degrees of librational motion.

At higher temperature, the nitroxide may exchange among the different local conformations and spend time undocked from the helix barrel. When extended into solution, the label tumbles anisotropically about its tether which corresponds approximately to the nitroxide *x* axis. Recently, Mchaourab *et al.* investigated Cys-SL side-chain dynamics in T4 lysozyme and proposed that the disulfide linker may be immobilized against the surface of solvent-exposed helices through van der Waals interactions (*38*). Such an interaction may occur between the 3K helix and the Cys-SL side chain (Fig. 1). However, this still allows for mobility about two sigma bonds connecting the disulfide and the nitroxide ring. Thus, their proposal is consistent with our observation of anisotropic motion.

Most previous studies on spin-labeled peptides have been performed at 9 GHz where unresolved hyperfine interactions from the nitroxide ring and methyl protons are comparable to the motion-dependent line broadening. These proton hyperfine couplings tend to mask the dynamical contribution. To address this problem, one must use deuterated nitroxides to eliminate inhomogeneous broadening or employ deconvolution techniques (*39*) to estimate the homogeneous, motion-dependent lineshape. In fact, simulation of 9-GHz spectra using isotropic and anisotropic motion obtained from best fit models of the 306-K data yielded spectra that were nearly superimposable with linewidths dominated by inhomogeneous broadening. At 139.5 GHz, the motionally narrowed spectral lines are predominantly homogeneous since secular broadening from **g** anisotropy is an order of magnitude greater than at 9 GHz and therefore overwhelms the inhomogeneous proton hyperfine interactions. Moreover, nonsecular relaxation processes (i.e., electron spin flips) are suppressed at high frequency (*23*). This suppression simplifies the expressions for the lineshape parameters (A, B, and C) thereby leading to more accurate estimates of τ_R and N. Nevertheless, the 9-GHz data may still provide useful information. Freed and co-workers have simultaneously analyzed the 9- and 250-GHz spectra of perdeuterated tempone (*23*) cholestane spin label (*40*) and found that models of fully anisotropic motion were required to fit the data. Our work on the spin-labeled 3K-11 peptide does not employ deuteration and, at correlation times typical for peptides in aqueous solution, the 9-GHz linewidths are dominated by inhomogeneous broadening. Thus, we prefer a conservative spectral analysis featuring only the high-frequency spectra.

These studies demonstrate the feasibility of performing high-frequency EPR on spin-labeled biomolecules in fluid aqueous solution. Barnes and Freed recently reported the development of an aqueous sample holder for 250-GHz EPR spectroscopy (*41*). They noted that 139.5-GHz EPR had only been performed on spin-labeled samples that were lyophilized, frozen, or partly humidified. This present work demonstrates clearly the feasibility of performing 139.5-GHz EPR on fluid aqueous samples. In addition, the sensitivity is comparable to that obtained by Barnes and Freed but without the development of specialized sample chambers.

High-frequency EPR offers significant advantages over conventional 9-GHz EPR. The sensitivity is sufficiently enhanced that experiments may be performed on a fraction of a microgram of spin-labeled peptide. In addition, inhomogeneous broadening from unresolved hyperfine couplings becomes small compared to the homogeneous linewidths. Thus, preparation of isotopically substituted nitroxides is not required for quantitative lineshape analysis. In addition, for correlation times less than 0.5 ns as are often found for peptides in aqueous solution, EPR spectra at 139.5 GHz are characterized by three minimally overlapped hyperfine lines and this greatly facilitates lineshape analysis. Finally, spectra at 139.5 GHz are more sensitive to anisotropic motion. This sensitivity should provide a deeper understanding of the local dynamics at the nitroxide attachment point.

ACKNOWLEDGMENTS

This work was supported by grants from the National Institutes of Health GM-46870 (G.L.M.), RR-00995 (R.G.G.), and GM-38352 (R.G.G. and D.J.S.) and by a grant from the National Science Foundation MCB 9408284 (G.L.M.). M. Bennati expresses her gratitude to the Deutsche Forschungsgemeinshaft for a postdoctoral grant. G.V.M. was supported by an NIH predoctoral fellowship (GM-16396) and G.J.G. was supported by an American Cancer Society postdoctoral fellowship (PF-3668).

REFERENCES

1. S. M. Miick, G. V. Martinez, W. R. Fiori, A. P. Todd, and G. L. Millhauser, Short alanine-based peptides may form 3_{10}-helices and not α-helices in aqueous solution [published correction appears in *Nature* 1995, **377,** 257], *Nature* **359,** 653–655 (1992).
2. W. R. Fiori, S. M. Miick, and G. L. Millhauser, Increasing sequence length favors α-helix over 3_{10}-helix in alanine-based peptides: Evidence for a length-dependent structural transition, *Biochemistry* **32,** 11957–11962 (1993).
3. W. R. Fiori, K. M. Lundberg, and G. L. Millhauser, A single carboxy-terminal arginine determines the amino-terminal helix conformation of an alanine-based peptide, *Nat. Struct. Biol.* **1,** 374–377 (1994).
4. G. L. Millhauser, Views of helical peptides—A proposal for the position of 3(10)-helix along the thermodynamic folding pathway, *Biochemistry* **34,** 3873–3877 (1995).
5. G. L. Millhauser, Selective placement of electron spin resonance spin labels: New structural methods for peptides and proteins, *Trends Biochem. Sci.* **17,** 448–452 (1992).
6. C. Altenbach and W. L. Hubbell, The aggregation state of spin-labeled melittin in solution and bound to phospholipid membranes: Evidence that membrane-bound melittin is monomeric, *Proteins* **3,** 230–242 (1988).
7. S. M. Miick, K. M. Casteel, and G. L. Millhauser, Experimental

molecular dynamics of an alanine-based helical peptide determined by spin label electron spin resonance, *Biochemistry* **32,** 8014–8021 (1993).

8. F. B. Sheinerman and C. L. Brooks, 3(10) Helices in peptides and proteins as studied by modified Zimm-Bragg theory, *J. Am. Chem. Soc.* **117,** 10098–10103 (1995).
9. W. S. Young and C. L. Brooks, A microscopic view of helix propagation—N and C-terminal helix growth in alanine helices, *J. Mol. Biol.* **259,** 560–572 (1996).
10. H. W. Long and R. Tycko, Biopolymer conformational distributions from solid-state NMR: Alpha-helix and 3(10)-helix contents of a helical peptide, *J. Am. Chem. Soc.* **120,** 7039–7048 (1998).
11. A. P. Todd and G. L. Millhauser, ESR spectra reflect local and global mobility in a short spin-labeled peptide throughout the α-helix $\rightarrow$ coil transition, *Biochemistry* **30,** 5515–5523 (1991).
12. C. Altenbach, T. Marti, H. G. Khorana, and W. L. Hubbell, Transmembrane protein structure: spin labeling of bacteriorhodopsin mutants, *Science* **248,** 1088–1092 (1990).
13. W. L. Hubbell and C. Altenbach, Investigation of structure and dynamics in membrane proteins using site-directed spin labeling, *Curr. Opin. Struct. Biol.* **4,** 566–573 (1994).
14. W. L. Hubbell, H. S. Mchaourab, C. Altenbach, and M. A. Lietzow, Watching proteins move using site-directed spin labeling, *Structure* **4,** 779–83 (1996).
15. Y. S. Lebedev, High-frequency and continuous-wave electron spin resonance, *in* "Modern Pulsed and Continuous-Wave Electron Spin Resonance" (L. Kevan and M. K. Bowman, Eds.), pp. 365–404, Wiley, New York (1990).
16. D. E. Budil, K. A. Earle, W. B. Lynch, and J. H. Freed, Electron paramagnetic resonance at 1 millimeter wavelengths, *in* "Advanced EPR: Applications in Biology and Biochemistry" (A. J. Hoff, Ed.) pp. 307–340, Elsevier, Amsterdam (1989).
17. L. J. Berliner, J. Grunwald, H. O. Hankovszky, and K. Hideg, A novel reversible thiol-specific spin label: Papain active site labeling and inhibition, *Anal. Biochem.* **119,** 450–455 (1982).
18. R. Koradi, M. Billeter, and K. Wuthrich, MOLMOL: A program for display and analysis of macromolecular structures, *J. Mol. Graphics* **14,** 51–55 (1996).
19. R. Sayle and E. J. Milner-White, RasMol: Biomolecular graphics for all, *Trends Biochem. Sci.* **20,** 374 (1995).
20. L. R. Becerra, *et al.,* A spectrometer for dynamic nuclear polarization and electron paramagnetic resonance at high frequencies, *J. Magn. Reson. A* **117,** 28–40 (1995).
21. A. Grupp and M. Mehring, Pulsed ENDOR spectroscopy in solids, *in* "Modern Pulsed and Continuous-Wave Electron Spin Resonance" (L. Kevan and M. K. Bowman, Eds.) pp. 195–229, Wiley–Interscience, New York (1990).
22. S. Un, J. Bryant and R. G. Griffin, Precision field-sweep system for superconducting solenoids and its application to high-frequency EPR spectroscopy, *J. Magn. Reson. A* **101,** 92–94 (1993).
23. D. E. Budil, K. A. Earle, and J. H. Freed, Full determination of the rotational diffusion tensor by electron paramagnetic resonance at 250 GHz, *J. Phys. Chem.* **97,** 1294–1303 (1993).
24. D. J. Schneider and J. H. Freed, Chapter 1: Calculating slow motional magnetic resonance spectra: A user's guide, *in* "Biological Magnetic Resonance: Spin Labeling Theory and Applications" (L. J. Berliner and J. Reuben, Eds.) Vol. 8, pp. 1–76, Plenum Press, New York (1989).
25. S. M. Miick and G. L. Millhauser, Rotational diffusion and intermolecular collisions of a spin labeled α-helical peptide determined by electron spin resonance spectroscopy, *Biophys. J.* **63,** 917–925 (1992).
26. W. H. Press, B. P. Flannery, S. A. Teukolsky, and W. T. Vetterling, "Numerical Recipes: The Art of Scientific Computing," Cambridge Univ. Press, Cambridge (1986).
27. P. Hanson, *et al.,* Electron spin resonance and structural analysis of water soluble, alanine-rich peptides incorporating TOAC, *Mol. Phys.* **95,** 957–966 (1998).
28. P. Hanson, G. Millhauser, F. Formaggio, M. Crisma, and C. Toniolo, ESR characterization of hexameric, helical peptides using double TOAC spin labeling, *J. Am. Chem. Soc.* **118,** 7618–7625 (1996).
29. P. Hanson, *et al.,* Distinguishing helix conformations in alanine-rich peptides using the unnatural amino acid TOAC and electron spin resonance, *J. Am. Chem. Soc.* **118,** 271–272 (1996).
30. C. Toniolo, *et al.,* Synthesis and conformational studies of peptides containing TOAC, a spin labeled $C^{\alpha,\alpha}$-disubstituted glycine, *J. Pept. Sci.* **1,** 45–57 (1995).
31. H. W. Spiess, Deuteron NMR—A new tool for studying chain mobility and orientation in polymers, *in* "Advances in Polymer Science" (H. H. Kausch and H. G. Zachmann, Eds.) Vol. 66, pp. 23–58, Springer-Verlag, Berlin (1985).
32. D. M. Rice, *et al.,* Rotational jumps of the tyrosine side chain in crystalline enkephalin. ^{2}H NMR line shapes for aromatic ring motion in solids, *J. Am. Chem. Soc.* **103,** 7707–7710 (1981).
33. D. M. Rice, Y. C. Meinwald, H. A. Scheraga, and R. G. Griffin, Tyrosyl motion in peptides: ^{2}H NMR line shapes and spin-lattice relaxation, *J. Am. Chem. Soc.* **109,** 1636–1640 (1987).
34. D. M. Rice, *et al.,* Solid state NMR investigations of lipid bilayers, peptides and proteins, *in* "Biomolecular Stereodynamics" (R. E. Sarma, Ed.) Vol. 2, pp. 255, Adenine Press, New York (1981).
35. R. G. Griffin, *et al.,* Deuterium NMR studies of dynamics in solids *in* (G. Long and F. Grandjean, Eds.), "Lecture Notes for the NATO-ASI: The Time Domain in Surface and Structural Dynamics," Il Ciocco, Italy (1987).
36. M. H. Frey, J. A. DiVerdi, and S. J. Opella, Dynamics of phenylalanine in the solid state by NMR, *J. Am. Chem. Soc.* **107,** 7311–7315 (1985).
37. H. J. Steinhoff and W. L. Hubbell, Calculation of electron paramagnetic resonance spectra from Brownian dynamics trajectories—Application to nitroxide side chains in proteins, *Biophys. J.* **71,** 2201–2212 (1996).
38. H. S. Mchaourab, M. A. Lietzow, K. Hideg, and W. L. Hubbell, Motion of spin-labeled side chains in T4 lysozyme, correlation with protein structure and dynamics, *Biochemistry* **35,** 7692–7704 (1996).
39. B. L. Bales, Inhomogeneously broadened spin-label spectra, *in* "Biological Magnetic Resonance: Spin Labeling Theory and Applications" (L. J. Berliner and J. Reuben, Eds.) Vol. 8, pp. 77–130, Plenum Press, New York (1989).
40. K. A. Earle, D. E. Budil, and J. H. Freed, 250-GHz EPR of nitroxides in the slow-motional regime—Models of rotational diffusion, *J. Phys. Chem.* **97,** 13289–13297 (1993).
41. J. Barnes and J. Freed, Aqueous sample holders for high-frequency electron spin resonance, *Rev. Sci. Instrum.* **68,** 2838–2846 (1997).
42. A. Capiomont, B. Chion, J. Lajzerowicz-Bonneteau, and H. Lemaire, Interpretation and utilization for crystal structure determination of ESR spectra of single crystals of nitroxide free radicals, *J. Chem. Phys.* **60,** 2530–2535 (1974).